

# Ionization Equilibria for Side-Chain Carboxyl Groups in Oxidized and Reduced Human Thioredoxin and in the Complex with Its Target Peptide from the Transcription Factor NF $\kappa$ B<sup>†</sup>

Jun Qin, G. Marius Clore,\* and Angela M. Gronenborn\*

Laboratory of Chemical Physics, Building 5, National Institute of Diabetes and Digestive and Kidney Diseases, National Institutes of Health, Bethesda, Maryland 20892-0520

Received September 26, 1995; Revised Manuscript Received November 9, 1995<sup>⊗</sup>

**ABSTRACT:** The pH dependence of the <sup>13</sup>C chemical shifts of the side-chain carboxyl carbons of all Asp and Glu residues in the reduced and oxidized states of human thioredoxin and in a mixed disulfide complex of human thioredoxin with a target peptide from the transcription factor NF $\kappa$ B has been investigated by multidimensional triple-resonance NMR spectroscopy. While the titration curves for most of the side-chain carboxyl resonances exhibit simple Henderson–Hasselbalch behavior with pK<sub>a</sub> values not far from those found for model compounds, several side chains give rise to two- or three-step titration curves, indicative of the influence of multiple ionizations. In particular, the triad formed by Asp58, Asp60, and Asp61 forms such a complex network of titrating groups. The ionization behavior of Asp26 shows an abnormally high pK<sub>a</sub> value for an aspartate residue in all states of human thioredoxin, with pK<sub>a</sub> values of 9.9 in the reduced state, 8.1 in the oxidized state, 8.9 in the mixed disulfide complex, and 8.6 in an active site mutant in which Cys35 was replaced by Ala. The unambiguous determination of the pK<sub>a</sub> values of Asp26 for a variety of states of human thioredoxin presented in this paper is highly significant in view of two recent reports on *Escherichia coli* thioredoxin which presented contradicting pK<sub>a</sub> values for Asp26 and Cys35 [Wilson et al. (1995) *Biochemistry* 34, 8931–8939; Jeng et al. (1995) *Biochemistry* 34, 10101–10105]. The stabilization of the protonated side chain of Asp26 in human thioredoxin is achieved via a hydrogen-bonding network involving the hydroxyl group of the neighboring Ser28 which is then connected to the active site region (comprising Cys32 and Cys35) via bound water molecules. The coupling of the buried Asp26 to the active site is responsible for the influence of the Asp26 ionization behavior on the titration shifts of active site residues.

Much effort has been directed at understanding electrostatic interactions in proteins and in particular their importance for binding, catalysis, and stability (Tanford, 1962; Matthew et al., 1985; Yang & Honig, 1992). In addition to numerous experimental studies, various models to evaluate electrostatic effects in proteins have been developed (Sharp & Honig, 1990; Bashford & Karplus, 1990; Warschel & Åquist, 1991; Allewell & Oberoi, 1991). NMR<sup>1</sup> provides a powerful method for the determination of pK<sub>a</sub> values of specific ionizable groups within a protein, and the ionization behavior of a large fraction of the ionizing groups for a number of proteins has been characterized by NMR (Ebina & Wüthrich, 1984; Kohda et al., 1991; Forman-Kay et al., 1992a; Bartik et al., 1994; Oda et al., 1994; Szyperski et al., 1994; Schaller & Robertson, 1995).

The focus of the present study is human thioredoxin (TRX), a small 12 kDa dithiol oxidoreductase which functions as a general reductant for disulfides in proteins (Holmgren, 1985, 1989) and has now been shown to play a critical role

in the regulation of several transcription factors (Abate et al., 1990; Toledano & Leonard, 1991; Matthews et al., 1992; Hayashi et al., 1993; Mitomo et al., 1994). The high-resolution three-dimensional solution structures of reduced and oxidized human TRX (Qin et al., 1994) and of a mixed disulfide complex of human TRX with a target peptide from the transcription factor NF $\kappa$ B (Qin et al., 1995) have been determined. In addition, a study on the ionization properties of reduced human TRX using 2D <sup>1</sup>H–<sup>15</sup>N and <sup>1</sup>H–<sup>1</sup>H correlation spectroscopy has been carried out previously (Forman-Kay et al., 1992a). The interpretation of pH-dependent chemical shifts of proton resonances adjacent to titrating groups (such as the  $\beta$ - and  $\gamma$ -methylenes of Asp and Glu, respectively) is challenging since the majority of titration curves do not exhibit classical sigmoidal Henderson–Hasselbalch behavior but display complex pH dependencies encompassing several inflection points (Forman-Kay et al., 1992a; Oda et al., 1994). This complexity arises from the exquisite sensitivity of proton chemical shifts to influences from additional carboxylates further away, as well as from other electronic and conformational factors, and highlights a drawback in their use for pK<sub>a</sub> determinations. The behavior observed for the proton resonances contrasts with that observed for side-chain carboxyl carbon resonances. The latter frequently exhibit simple sigmoidal Henderson–Hasselbalch titration curves between the deprotonated and protonated states of the carboxyl group with the ionized form

<sup>†</sup> This work was supported by the AIDS Targeted Anti-Viral Program of the Office of the Director of the National Institutes of Health (to G.M.C. and A.M.G.).

\* Authors to whom correspondence should be addressed.

<sup>⊗</sup> Abstract published in *Advance ACS Abstracts*, December 15, 1995.

<sup>1</sup> Abbreviations: NMR, nuclear magnetic resonance; TRX, thioredoxin; 2D, two dimensional; 3D, three dimensional; CT-HCACO, constant time proton to directly bonded carbon to carbonyl correlation; HOHAHA, homonuclear Hartmann–Hahn spectroscopy; *E. coli*, *Escherichia coli*.

generally resonating  $\sim 3$  ppm upfield from the neutral form (Oda et al., 1994; Yamazaki et al., 1994). We have therefore used multidimensional triple-resonance NMR spectroscopy to correlate the carboxyl carbon side-chain resonances of Asp and Glu with the  $\beta$ - and  $\gamma$ -methylene proton resonances, respectively, as a function of pH in order to determine the  $pK_a$  values for all aspartate and glutamate carboxyl groups in the reduced and oxidized states of human thioredoxin and in the mixed disulfide complex with the target peptide from NF $\kappa$ B. These experimental  $pK_a$  values are discussed in the light of the structural environment around the titrating side-chain groups. Of particular interest is Asp26, which is highly conserved in all thioredoxins and is thought to play a role in the control of the redox potential of *Escherichia coli* thioredoxin (Dyson et al., 1991; Langsetmo et al., 1991a,b). The importance of establishing the correct value for the  $pK_a$  of Asp26 has taken on new importance since two recent publications on *Escherichia coli* TRX have come to contradicting views as to the assignment of the  $pK_a$  values for Asp26 and Cys35 (Wilson et al., 1995; Jeng et al., 1995). Establishing the correct  $pK_a$  values for these groups is crucial for understanding the catalytic mechanism of disulfide bridge reduction by TRX.

## EXPERIMENTAL PROCEDURES

**Sample Preparation.** Expression and purification for the different protein variants of human TRX were identical to those used previously (Forman-Kay et al., 1992b; Qin et al., 1994, 1995), and uniform labeling with  $^{15}\text{N}$  and  $^{13}\text{C}$  was carried out by growing the bacteria in minimal medium with  $^{15}\text{NH}_4\text{Cl}$  and  $[^{13}\text{C}_6]\text{glucose}$  as the sole nitrogen and carbon sources, respectively. The titration studies on the oxidized and reduced forms of human TRX were carried out using the triple cysteine mutant (C62A, C69A, C73A) in which the three additional cysteines not involved in the redox reaction were replaced by alanines. It has been shown previously (Forman-Kay et al., 1992b; Qin et al., 1994) that this mutant is basically indistinguishable from wild-type human thioredoxin with respect to biological activity, overall structure, and stability. However, the advantage of the triple (C62A, C69A, C73A) mutant is that it circumvents any problems arising from intermolecular disulfide bond formation by the three free nonactive site cysteine residues upon oxidation, thereby enabling the oxidized state to be studied by NMR. The complex between the (C35A, C62A, C69A, C73A) mutant of human TRX and the 13-residue target peptide from NF $\kappa$ B (encompassing residues 56–68 of the p50 subunit) was prepared as described by Qin et al. (1995). Throughout the paper, we refer to the triple (C62A, C69A, C73A) and quadruple (C35A, C62A, C69A, C73A) mutants as human TRX and as the C35A mutant, respectively.

**NMR Spectroscopy.** All NMR experiments were carried out at 25 °C on either a Bruker AMX600 or AMX500 spectrometer equipped with a z-shielded gradient triple-resonance probe. The carboxyl side-chain carbons of Asp (Asn) and Glu (Gln) were correlated with their  $\beta$ - and  $\gamma$ -methylene proton resonances using a modified version (Yamazaki et al., 1994) of the constant time HCACO experiment (Powers et al., 1991). The pH dependence of the chemical shifts of the  $\text{C}^\alpha\text{H}$  and  $\text{C}^\beta\text{H}$  resonances of Ser28 and Cys32 was followed by means of 2D HOHAHA (Bax,

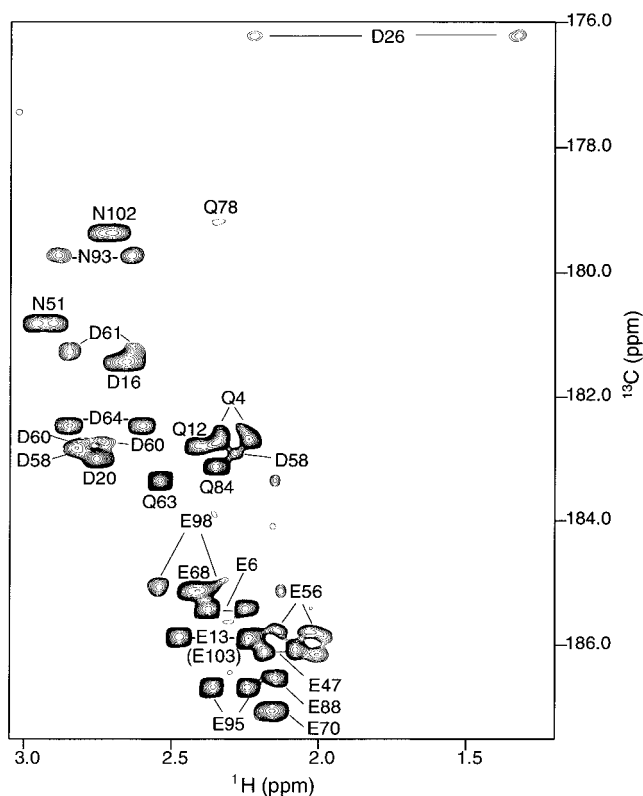


FIGURE 1:  $^{13}\text{C}$  ( $F_1$  axis)— $^1\text{H}$  ( $F_2$  axis) region of the 2D CT-HCACO experiment of oxidized human TRX at 25 °C and pH 5.5. The assignments of all Glu/Gln and Asp/Asn  $\text{C}^\beta$ — $\text{C}^\gamma\text{H}_2$  and  $\text{C}^\gamma$ — $\text{C}^\beta\text{H}_2$  correlations, respectively, are indicated.

1989) spectroscopy. The NMR spectra were processed with the NmrPipe package (Delaglio et al., 1995) and displayed and analyzed using the programs PIPP, CAPP, and STAPP (Garrett et al., 1991). Assignments were taken from previous work (Qin et al., 1994, 1995).

**pH Titrations.** Chemical shifts of the carboxyl carbon resonances were followed for samples containing approximately 1 mM protein in 100 mM sodium phosphate buffer. The pH was adjusted by the additions of small amounts of concentrated DCl or NaOD. The measured pH was not corrected for the isotope effect on the glass electrode, and measurements were taken before and after the NMR experiment. The carbon shifts were referenced with respect to 3-(trimethylsilyl)propanoic- $d_4$  acid.

**Analysis of pH Titration Curves.**  $pK_a$  values were determined from the titration curves by a nonlinear least-squares fit of the data to the Henderson–Hasselbalch equation. In those cases where the titration curves could not be fit by the simple one  $pK_a$  Henderson–Hasselbalch equation, the data were fit to a noninteracting multiple  $pK_a$  model derived as a simple extension of the Henderson–Hasselbalch equation and given by eq 4 in Forman-Kay et al. (1992a). In these cases all the relevant titration curves were fit simultaneously. Nonlinear least-squares fitting was performed using the program FACSIMILE (Chance et al., 1977). The errors in the fitted parameters were obtained from conventional analysis of the variance–covariance matrix generated by the nonlinear least-squares optimization routine (Chance et al., 1977; Clore, 1983). It should be noted that these errors relate to the precision of the fitted parameters rather than to their accuracy (which may be additionally influenced by the presence of systematic errors which cannot

Table 1:  $pK_a$  Values of Asp and Glu Residues of Reduced and Oxidized Human TRX and of the Mixed Disulfide Complex of the C35A Mutant with the NF $\kappa$ B Target Peptide, Derived by Monitoring the pH Dependence of the Chemical Shifts of the Carboxyl Carbon Resonances Using 2D CT-HCACO Spectroscopy<sup>a</sup>

	reduced			oxidized			complex		
	$pK_a$	$\delta_{low}$	$\delta_{high}$	$pK_a$	$\delta_{low}$	$\delta_{high}$	$pK_a$	$\delta_{low}$	$\delta_{high}$
Asp16	4.0 ± 0.06	178.5	181.7	4.2 ± 0.03	178.5	181.7	4.0 ± 0.09	178.5	181.7
Asp20	3.8 ± 0.05	179.6	183.1	3.8 ± 0.03	179.5	183.1	3.6 ± 0.04	179.5	183.1
Asp26	9.9 ± 0.1	175.5	181.6	8.1 ± 0.02	176.2	180.4	8.9 ± 0.3	175.8	180.0
Asp64	3.2 ± 0.06	179.6	182.5	3.2 ± 0.05	179.3	182.6	2.7 ± 0.05	178.6	182.4
Glu6	4.8 ± 0.08	182.2	186.1	4.9 ± 0.04	182.2	186.1	4.9 ± 0.03	182.2	186.4
Glu13	4.4 ± 0.07	182.0	186.4	4.4 ± 0.07	181.9	186.3	4.3 ± 0.09	181.8	186.4
Glu47	4.1 ± 0.1	182.1	185.9	4.3 ± 0.05	182.0	186.0	4.1 ± 0.05	181.9	185.9
Glu56 <sup>b</sup>	3.1 ± 0.04	181.2	186.5	3.2 ± 0.05	181.5	186.5	3.1 ± 0.02	181.1	186.4
	5.0 ± 0.1	185.0 <sup>c</sup>		5.1 ± 0.08	185.0 <sup>c</sup>		4.8 ± 0.07	185.0 <sup>c</sup>	
Glu68	4.9 ± 0.07	181.7	186.4	5.1 ± 0.04	181.4	186.3	4.9 ± 0.05	181.5	186.4
Glu70	4.6 ± 0.08	182.9	187.9	4.8 ± 0.05	183.0	187.8	4.5 ± 0.07	182.8	187.9
Glu88	3.7 ± 0.08	183.0	186.8	3.6 ± 0.05	182.8	186.7	3.4 ± 0.05	182.8	186.5
Glu95	4.1 ± 0.02	182.2	186.9	4.1 ± 0.04	182.3	186.8	3.8 ± 0.04	182.2	186.9
Glu98	3.9 ± 0.02	182.0	185.3	3.9 ± 0.04	182.1	185.2	3.8 ± 0.05	182.0	185.3
Glu103	4.4 ± 0.07	182.0	186.4	4.5 ± 0.06	182.0	186.5	4.3 ± 0.09	181.8	186.4

<sup>a</sup> Except for Glu56, all titration curves were fit to a single  $pK_a$ , optimizing the value of the  $pK_a$  and the  $^{13}C$  chemical shifts (in ppm) of the side-chain carboxyl carbon in the fully protonated ( $\delta_{low}$ ) and fully unprotonated ( $\delta_{high}$ ) states. With the exception of the value of  $\delta_{high}$  for Asp26 in the reduced state of human TRX, the errors in the chemical shift values are less than 0.1 ppm and in the majority of cases less than 0.07 ppm. The error in the value of  $\delta_{high}$  for Asp26 in the reduced state is  $\pm 0.25$  ppm. The data for Asp58, Asp60, and Asp61 are not included in this table as their titration curves required a three  $pK_a$  fit which is reported in Table 2. It should be noted that the errors in the fitted parameters ( $pK_a$ 's and chemical shifts) relate to their precision as derived from an analysis of the variance-covariance matrix generated by the Powell nonlinear least-squares optimization routine (Chance et al., 1977; Clore, 1983). The accuracy of the fitted parameters, however, will always be somewhat lower than their precision, due to the potential presence of unknown systematic errors which cannot be assessed and uncertainties in the choice of model used to fit the data. <sup>b</sup> In the case of Glu56, a two  $pK_a$  model was required to fit the data, optimizing the value of the two  $pK_a$  values and the  $^{13}C$  carboxyl carbon chemical shifts at low, intermediate, and high pH. <sup>c</sup> The intermediate chemical shifts for the two  $pK_a$  fits to the titration curves of Glu56.

be assessed, as well as by the choice of the model used to fit the data).

## RESULTS AND DISCUSSION

Titration curves for the carboxyl groups of all Asp and Glu residues were followed using a modified 2D version of the CT-HCACO experiment, and a representative spectrum for the oxidized state of human TRX displaying the region of the side-chain carboxyl and carbonyl carbons is shown in Figure 1. Cross peaks are observed between the C $\gamma$ O carbon and the adjacent  $\beta$ -methylene protons (separated by two bonds) in the case of Asp and Asn and between the C $\delta$ O carbon and the adjacent  $\gamma$ -methylene protons in the case of Glu and Gln. Based on the previously established assignments of the  $\beta$ - and  $\gamma$ -methylene proton resonances and the  $^{13}C$   $\alpha$ -,  $\beta$ -, and  $\gamma$ -carbon resonances (Qin et al., 1994, 1995), the side-chain carbonyl and carboxyl carbon resonances were first assigned unambiguously using a modified 3D version of the CT-HCACO experiment. Titration curves were obtained for all Asp and Glu residues in oxidized, reduced, and complexed human TRX, and the  $pK_a$  values are summarized in Tables 1 and 2. Titration curves for the oxidized state of human TRX are presented in Figure 2, and it is apparent that the majority of the carboxylates titrate with a single  $pK_a$  exhibiting classical Hendersen-Hasselbalch behavior. The exceptions are the carboxylates of Asp58, Asp60, Asp61, and Glu56 which display more complex behavior discussed below.

Asp16, Asp20, and Asp64 can be viewed as representatives of surface amino acids which titrate in a manner similar to that of an Asp of a small random coil peptide. These three residues have  $pK_a$  values of 4.2, 3.8, and 3.2, respectively, close to that reported for model compounds (3.9–4.0; Creighton, 1993) and other reported surface aspartates (3.2–

Table 2:  $pK_a$  Values of the Asp58, Asp60, and Asp61 Triad in Reduced and Oxidized Human TRX and in the Mixed Disulfide Complex of the C35A Mutant with the NF $\kappa$ B Target Peptide, Derived by Monitoring the pH Dependence of the Chemical Shifts of the Carboxyl Carbon Resonances Using 2D CT-HCACO Spectroscopy<sup>a</sup>

	reduced	oxidized	complex
$pK_{a1}$	2.8 ± 0.1	2.7 ± 0.06	2.0 ± 0.05
$pK_{a2}$	4.2 ± 0.2	3.9 ± 0.1	3.3 ± 0.1
$pK_{a3}$	5.3 ± 0.3	5.2 ± 0.1	4.7 ± 0.1
Asp58			
$\delta_{low}$	180.2 ± 0.08	180.3 ± 0.04	180.2 ± 0.04
$\delta_{int1}$	181.7 ± 0.25	181.1 ± 0.09	182.0 ± 0.05
$\delta_{int2}$	183.0 ± 0.11	182.2 ± 0.07	182.6 ± 0.04
$\delta_{high}$	183.1 ± 0.04	183.2 ± 0.02	183.0 ± 0.02
Asp60			
$\delta_{low}$	178.9 ± 0.06	178.7 ± 0.07	178.8 ± 0.05
$\delta_{int1}$	181.5 ± 0.36	181.4 ± 0.16	181.5 ± 0.07
$\delta_{int2}$	182.8 ± 0.12	182.2 ± 0.07	182.7 ± 0.05
$\delta_{high}$	183.1 ± 0.04	183.0 ± 0.02	183.2 ± 0.02
Asp61			
$\delta_{low}$	178.8 ± 0.04	178.7 ± 0.02	178.8 ± 0.02
$\delta_{int1}$	179.3 ± 0.36	179.1 ± 0.16	178.9 ± 0.07
$\delta_{int2}$	180.9 ± 0.16	180.4 ± 0.10	180.4 ± 0.05
$\delta_{high}$	181.8 ± 0.04	181.8 ± 0.02	181.8 ± 0.02

<sup>a</sup> For each state of human TRX, the titration curves for the C $\delta$  carboxyl carbon atoms of the three aspartate residues were fit simultaneously by optimizing the three  $pK_a$  values and the values of the low ( $\delta_{low}$ ), two intermediate ( $\delta_{int1}$ ,  $\delta_{int2}$ ), and high ( $\delta_{high}$ ) pH [ $^{13}C$ ]carboxyl carbon chemical shifts (in ppm) for each curve.

4.2; Kohda et al., 1991; Oda et al., 1994; Szyperski et al., 1994; Oliveberg et al., 1995).

Asp26 exhibits an unusual titration curve such that in the case of the oxidized protein no titration shift is observed from pH 2 up to about pH 7. The  $pK_a$  value determined for oxidized human TRX is 8.1. In the reduced protein Asp26 has an even higher  $pK_a$  value of 9.9. In our previous titration

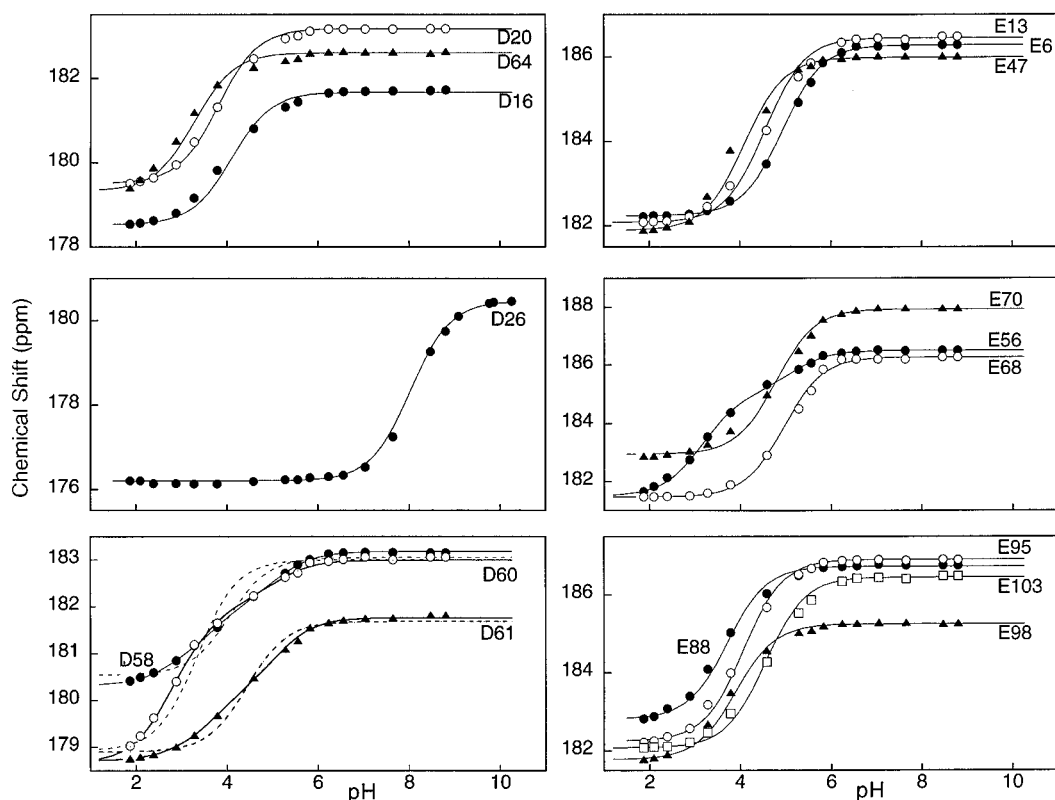


FIGURE 2: Chemical shift titration curves for the  $^{13}\text{C}$ carboxyl resonances of all Asp and Glu residues of oxidized human TRX in the pH range 1.9–10. The solid lines represent least-squares best fits to the data. With the exception of the curves for Asp58, Asp60, Asp61, and Glu56, all the curves were fitted to the classical single  $pK_a$  Henderson–Hasselbalch equation. For Asp58, Asp60, and Asp61, the data for all three residues were fitted simultaneously using a noninteracting three  $pK_a$  model (solid line). The dotted lines for these three residues represent least-squares fits to a single  $pK_a$  model illustrating the large deviations from classical Henderson–Hasselbalch behavior. The titration curve for Glu56 was fitted with a noninteracting two  $pK_a$  model (solid line).

studies on reduced wild-type human TRX (Forman-Kay et al., 1992a) the  $pK_a$  of Asp 26 was not determined accurately since the protein starts to unfold at these high pH values and a large number of changes occur in the 2D  $^1\text{H}$ – $^1\text{H}$  correlation spectra. We therefore stated at the time that Asp26 did not titrate within the normal pH range (Forman-Kay et al., 1992a). From all the data presently available in our laboratory on reduced human TRX ( $pK_a = 9.9$ ), oxidized human TRX ( $pK_a = 8.1$ ), the mixed disulfide complex between human TRX and the NF $\kappa$ B peptide ( $pK_a = 8.9$ ), and the C35A mutant of human TRX ( $pK_a = 8.6$ ), it is clear that Asp26 titrates with an extraordinarily high  $pK_a$  value in all states of human TRX. These findings are consistent with the report by Wilson et al. (1995), who determined a  $pK_a > 9$  for Asp26 in the reduced state of *Escherichia coli* TRX. Our results and those of Wilson et al. (1995), on the other hand, are in direct contrast to the interpretation recently put forward by Jeng et al. (1995), who attributed a  $pK_a$  of 7.4 to Asp26 in the reduced state of *E. coli* TRX and assigned the high  $pK_a$  value of  $>9$  to the thiol of Cys35.

We believe that the assignment of  $pK_a$  values for Asp26 and Cys35 put forward by Jeng et al. (1995) is highly unlikely since it is based primarily on  $^1\text{H}$  and  $^{13}\text{C}$  shifts of atoms in the  $\beta$  position of the cysteines. As noted in the introduction, it is extremely difficult to extract  $pK_a$  values from titration curves that deviate from classical Henderson–Hasselbalch behavior, and indeed this is precisely the nature of the curves observed for the  $\beta$  positions. We too found complicated titration behavior for the active site residues, including Cys32 and Cys35 (Forman-Kay et al., 1992a), and several  $pK_a$ 's contributed to the observed titration curves.

We attributed a  $pK_a$  of 6.3 to Cys32, while the  $pK_a$  value for Cys35 could not be accurately determined and was tentatively assigned to lie within the range 7.5–8.6. With the availability of the C35A mutant, we reinvestigated the active site titration behavior. The proton titration curves for several pertinent resonances are displayed in Figure 3, and the results are summarized in Table 3. Although less complicated than the titration curves observed previously for the wild-type protein (Forman-Kay et al., 1992a), mainly due to the absence of one of the interacting titratable groups (i.e., Cys35), the titration curves for the  $\text{H}^\alpha$  and  $\text{H}^\beta$  resonances of Cys32 necessitated a two  $pK_a$  fit with  $pK_a$  values of 7.1 and 8.6. The  $pK_a$  of 8.6 clearly cannot arise from Cys35 since this residue is no longer present. Hence, this  $pK_a$  has to be assigned to the buried Asp26. This is confirmed by the  $pK_a$  of 8.9 derived from the titration curve of the carboxyl side-chain carbon of Asp26 in the mixed disulfide complex of the C35A mutant and the NF $\kappa$ B peptide. Further substantiation is provided by the titration behavior of the proton resonances of Ser28. In human TRX the hydroxyl  $\text{O}^1\text{H}$  of Ser28 is hydrogen bonded to the side-chain carboxyl group of Asp26 (Qin et al., 1994). Consequently, any titration observed for the proton resonances of Ser28 should reflect the ionization behavior of Asp26. As is evident from the data presented in Figure 3 and Table 3, the two  $pK_a$  values derived from the titration curves for the proton resonances of Ser28 and Cys32 in the C35A mutant of human TRX clearly reflect the ionization of both the cysteine thiol of Cys32 and the carboxylate of the buried Asp26. It is interesting to note that substitution of Cys35 by Ala slightly raises the  $pK_a$  of Cys 32 from 6.3 to 7.1, which is still clearly

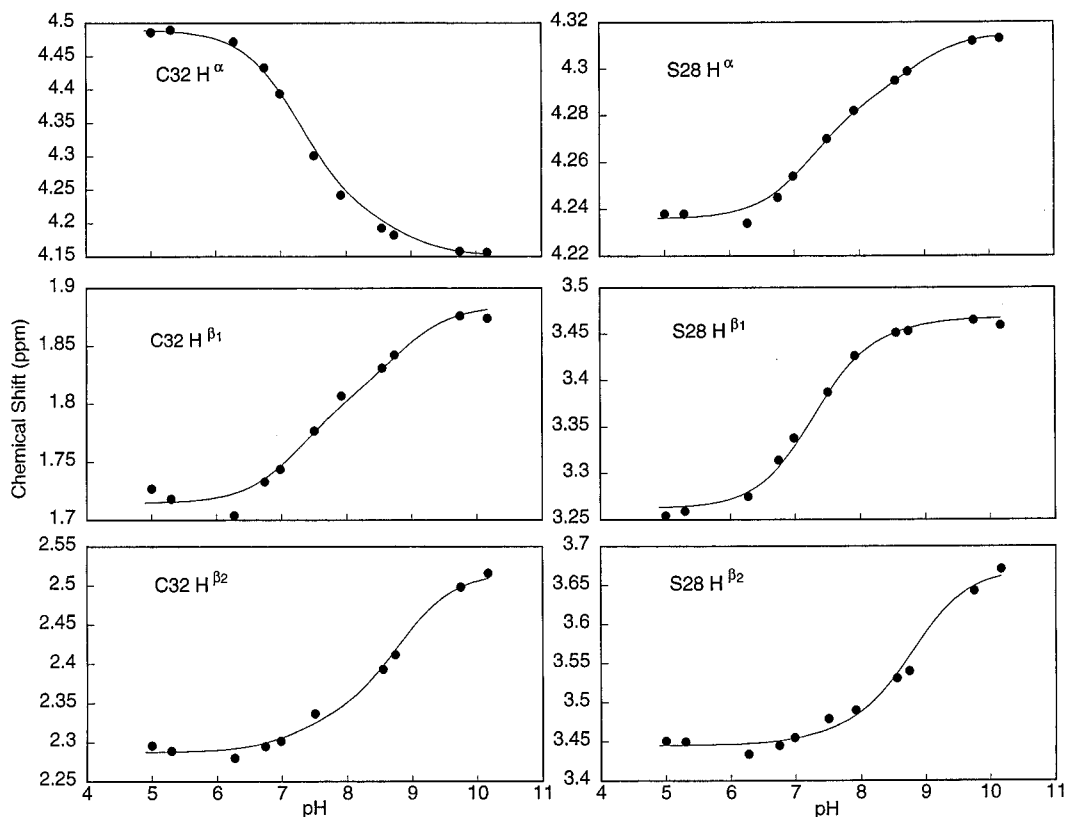


FIGURE 3: Chemical shift titration curves for the  $C^{\alpha}H$  and  $C^{\beta}H$  resonances of Cys32 and Ser28 for the C35A mutant of human TRX. All six curves were fitted simultaneously to a noninteracting two  $pK_a$  model (solid lines). These data were obtained from a series of 2D  $^1H$ - $^1H$  HOHAHA spectra.

Table 3: Titration Behavior of Cys32 and Ser28 in the C35A Mutant of Human Thioredoxin<sup>a</sup>

	$\delta_{low}$ (ppm)	$\delta_{int}$ (ppm)	$\delta_{high}$ (ppm)
	$pK_{a1} = 7.1 \pm 0.09$ ; $pK_{a2} = 8.6 \pm 0.10$		
Cys32			
$H^{\alpha}$	$4.49 \pm 0.008$	$4.26 \pm 0.011$	$4.15 \pm 0.008$
$H^{\beta1}$	$1.72 \pm 0.004$	$1.78 \pm 0.007$	$1.89 \pm 0.005$
$H^{\beta2}$	$2.28 \pm 0.005$	$2.34 \pm 0.009$	$2.50 \pm 0.007$
Ser28			
$H^{\alpha}$	$4.24 \pm 0.008$	$4.27 \pm 0.017$	$4.32 \pm 0.010$
$H^{\beta1}$	$3.26 \pm 0.013$	$3.44 \pm 0.025$	$3.47 \pm 0.017$
$H^{\beta2}$	$3.44 \pm 0.011$	$3.46 \pm 0.02$	$3.65 \pm 0.014$

<sup>a</sup> The titration curves for the  $H^{\alpha}$  and methylene protons of Ser28 and Cys32, derived by monitoring the pH dependence of their chemical shifts using 2D HOHAHA spectroscopy, were fit simultaneously to a noninteracting two  $pK_a$  model by optimizing the value of  $pK_{a1}$  and  $pK_{a2}$  and the low ( $\delta_{low}$ ), intermediate ( $\delta_{int}$ ), and high ( $\delta_{high}$ ) chemical shifts. The  $pK_{a2}$  value of 8.6 reflects the  $pK_a$  of the carboxylate of Asp26 (see Table 1).

well below that of a solvent-exposed thiol of 9.0–9.5 (Creighton, 1993). Thus, the proposal put forward for *Escherichia coli* TRX by Jeng et al. (1995) that the two cysteines in the active site share a proton, resulting in the lowered  $pK_a$  for Cys 32, cannot be valid for human TRX.

The titration data for the three remaining aspartates, Asp58, Asp60, and Asp61 (Figure 2), exhibit significant deviations from classical Henderson–Hasselbalch behavior. All three amino acids are located in close spacial proximity so that their ionizations reflect mutual influences. Specifically, the  $C^{\gamma}$ – $C^{\gamma}$  distance between Asp58 and Asp60, Asp58 and Asp61, and Asp60 and Asp61 is 4.8–4.9, 5.0, and 6.4 Å, respectively, in both the reduced and oxidized states. The corresponding distances in the mixed disulfide complex with

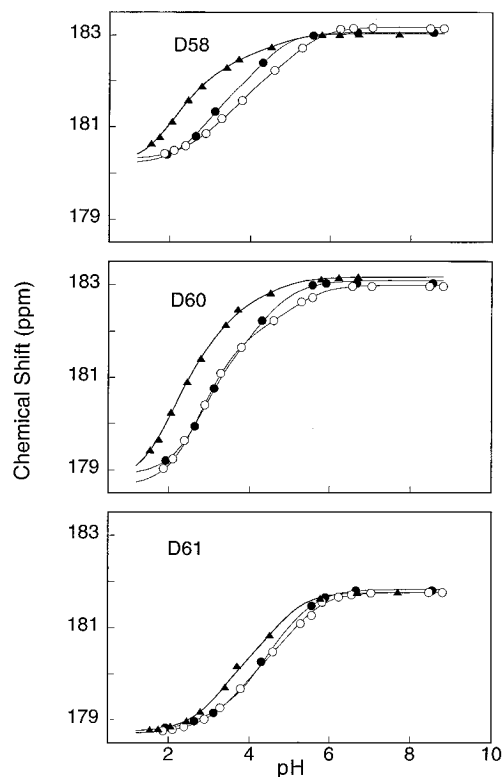


FIGURE 4: pH dependence of the  $[^{13}C]$ carboxyl chemical shifts of Asp58, Asp60, and Asp61 for human TRX in the reduced (●), oxidized (○), and complexed (▲) states. In each state, all three titration curves were fitted simultaneously using a noninteracting three  $pK_a$  model (solid lines).

the NF $\kappa$ B target peptide are 5.3, 4.4, and 6.2 Å, respectively. We therefore fit all three titration curves simultaneously using

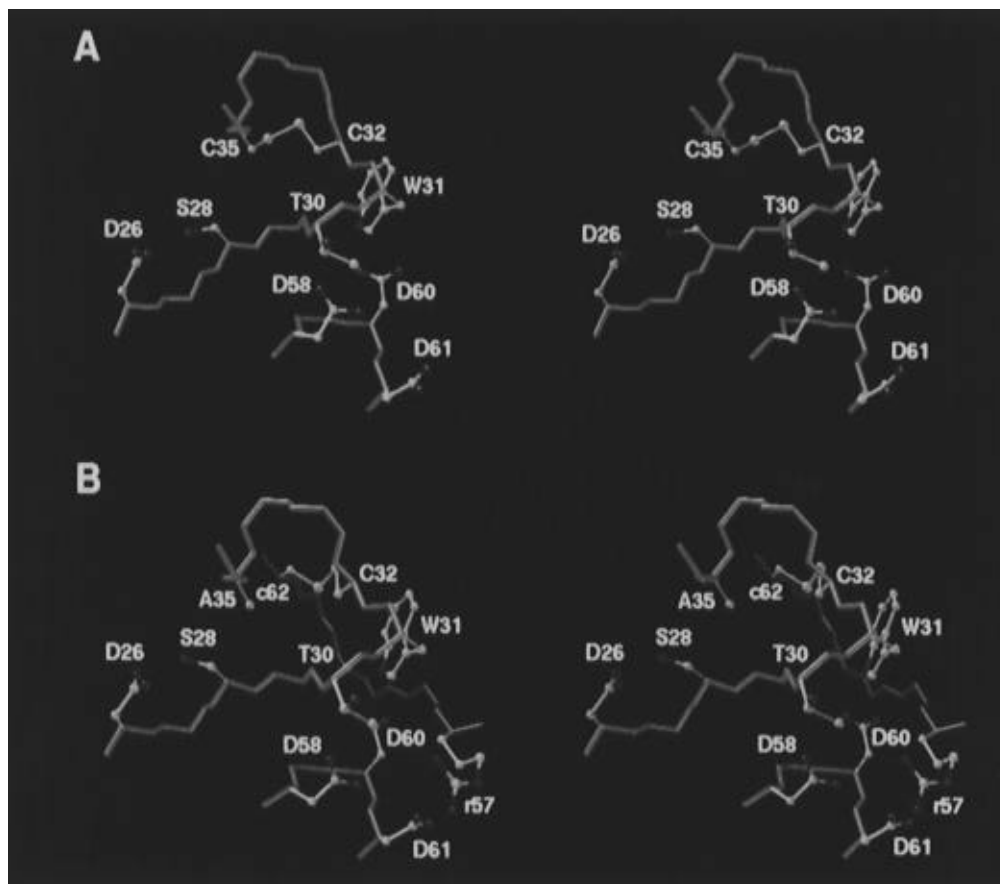


FIGURE 5: Stereoviews of the active site region of (A) oxidized human TRX and (B) the mixed disulfide intermediate complex of the C35A mutant with the NF $\kappa$ B peptide. The interaction of Asp26 with Ser28 and its proximity to the active site region are illustrated, and the close spatial proximity between Asp58, Asp60, and Asp61 and their interaction with Thr30 and Trp31 are highlighted. The polypeptide backbone of the protein is shown in green, and in (B) the backbone of the NF $\kappa$ B peptide is shown in red. In (B) the side chains of Arg57 and Cys62 of the peptide are labeled in lower case.

a three  $pK_a$  fit, and the results are summarized in Figure 4 and Table 2. While there is little difference in the titration behavior of these three residues in the reduced and oxidized states of human TRX, a substantial shift to lower  $pK_a$  values is observed in the complex with the NF $\kappa$ B target peptide. In fact, these changes in  $pK_a$  values are the largest observed between free human TRX (reduced or oxidized) and the mixed disulfide complex. In the three-dimensional structure of human TRX, Asp58 is positioned at the end of strand  $\beta_3$ , and both Asp60 and Asp61 are located in the turn connecting strand  $\beta_3$  and helix  $\alpha_3$ . This region is in close spatial proximity to the polypeptide chain immediately preceding the active site region (residues 32–35), and hydrogen bonds are present between the carboxylate of Asp58 and the backbone NH of Thr30 and between the carboxylate of Asp60 and the N $^{\epsilon}$ H of the indole ring of Trp31. As is evident from the structural comparison shown in Figure 5, the bound NF $\kappa$ B peptide interacts intimately with this highly charged region of the protein, and the interaction between the guanidinium group of Arg57 of the peptide with the entire network of negative charges set up by the three carboxylates of Asp58, Asp60, and Asp61 from the protein contributes to the stability of the complex and is responsible for the lowering of the associated  $pK_a$  values.

In addition to the seven aspartates, human TRX contains ten glutamates, the majority of which exhibit simple Henderson–Hasselbalch titration curves (Figure 2). Only Glu56 necessitated the use of a two  $pK_a$  fit to satisfactorily reproduce its titration curve. The  $pK_a$  values for all other

glutamates lie within the range of 3.6–4.9 for oxidized TRX with only small changes in the reduced form and the complex. The intrinsic  $pK_a$  value for a free glutamic acid lies in the range 4.3–4.5 (Creighton, 1993), and  $pK_a$  values for exposed glutamates have been reported in the range 3.9–4.4 (Oda et al., 1994; Szyperski et al., 1994; Schaller & Robertson, 1995; Oliveberg et al., 1995). Solvent-accessible side chains in the three-dimensional structure of human TRX comprise Glu6, Glu13, Glu47, Glu70, Glu88, Glu95, Glu98, and Glu103, all of which exhibit only marginally perturbed  $pK_a$  values. Both Glu6 and Glu68 exhibit somewhat elevated  $pK_a$  values of 4.8–4.9 and 4.9–5.1, respectively. One possible reason for an elevated  $pK_a$  value could be an area of strongly negative charge around the titratable group. In the case of Glu6 this strongly negative electrostatic region is due to the triad of Asp58, Asp60, and Asp61; in the case of Glu68, this residue is positioned in an area of negative charge arising from Asp64 and Glu70 located on either side of Glu6. The above reasoning is clearly supported by examining the electrostatic potential on the surface of the protein using the program Grasp (Nicholls et al., 1991). Glu56 exhibited abnormal behavior insofar that a two  $pK_a$  fit was necessary to reproduce its titration behavior. An explanation for this unusual behavior may be the fact that Glu56 is in close proximity to the cluster of interacting negative charges comprising Asp58, Asp60, and Asp61. The carboxylate of Glu56 is within 7 Å of that of Asp58, and both side chains are relatively surface inaccessible so that it is very likely that a mutual influence will be felt by the

titrating carboxylates. Indeed, the values of  $pK_{a2}$  for Glu56 in the three states of human TRX (Table 1) are very similar to those obtained independently for  $pK_{a3}$  of the Asp58, Asp60, and Asp61 triad (Table 2).

## CONCLUDING REMARKS

Using the constant time HCACO experiment, it was possible to directly follow the ionization shifts of the carboxyl carbons of all Asp and Glu residues of human TRX in a variety of states (reduced, oxidized, and in a mixed disulfide complex with a target peptide from NF $\kappa$ B). In this manner problems associated with monitoring  $^1\text{H}$  or  $^{13}\text{C}$  shifts of more remote atoms of the side chains, which often render the interpretation of titration curves challenging if not impossible, were circumvented, and unambiguous determinations of  $pK_a$  values could be obtained. The results establish unequivocally that Asp26 is protonated in all states of folded human TRX, exhibiting an unusually high  $pK_a$  value of 9.9 in the reduced state. This finding supports a similar observation and interpretation for the equivalent buried aspartate in *E. coli* TRX (Wilson et al., 1995) and casts doubt on an alternative interpretation by Feng et al. (1995). In this regard it is interesting to note that another protonated buried aspartate residue was recently identified in a HIV-1 protease inhibitor complex and shown to exhibit a  $pK_a$  value of  $>7.5$  (Yamazaki et al., 1994). The stabilization of the protonated side chain of Asp26 in human TRX is achieved via a hydrogen-bonding network involving the hydroxyl group of the neighboring Ser28 which is then connected to the active site region (comprising Cys32 and Cys35) via bound water molecules. Such water molecules connecting the carboxylate of Asp26 to the surface of the protein have been observed in the X-ray structures of *E. coli* and *Anabena* TRX (Katti et al., 1990; Saarinen et al., 1995) as well as in the NMR structures of reduced and oxidized human TRX (Qin et al., 1994). It is this tethering of the buried Asp26 to the active site which is responsible for the reflection of the Asp26 ionization behavior in the titration shifts of active site residues, in particular the  $\beta$ -positions of Cys35.

## ACKNOWLEDGMENT

We thank Dan Garrett and Frank Delaglio for software support, Rolf Tschudin for hardware support, and J. Huth and W. M. P. Kennedy for help with sample preparation.

## REFERENCES

Abate, C., Patel, L., Rauscher, F. J., & Curran, T. (1990) *Science* 249, 1157–1161.  
 Allewell, N. M., & Oberoi, H. (1991) *Methods Enzymol.* 202, 3–19.  
 Bartik, K., Redfield, C., & Dobson, C. M. (1994) *Biophys. J.* 66, 1180–1184.  
 Bashford, D., & Karplus, M. (1990) *Biochemistry* 29, 10219–10225.  
 Bax, A. (1989) *Methods Enzymol.* 176, 151–158.  
 Chance, E. M., Curtis, A. R., Jones, I. P., & Kirby, C. R. (1977) *FACSIMILE: A Computer Program for Flow and Chemistry Simulation and General Initial Value Problems*, Report No. AERE-R 8775, United Kingdom Atomic Energy Research Establishment (A.E.R.E.), Harwell.

Clore, G. M. (1983) in Report No. AERE-R 8775 (Garrett, M. J., & Barrett, A. N., Eds.) pp 313–348, Elsevier North-Holland, Amsterdam.  
 Creighton, T. E. (1993) *Proteins*, W. H. Freeman & Co., New York.  
 Delaglio, F., Grzesiek, S., Vuister, G., Zhu, G., Pfeifer, J., & Bax, A. (1995) *J. Biomol. NMR* (in press).  
 Dyson, H. J., Tennant, L. L., & Holmgren, A. (1991) *Biochemistry* 30, 4262–4268.  
 Ebina, S., & Wüthrich, K. (1984) *J. Mol. Biol.* 179, 283–288.  
 Forman-Kay, J. D., Clore, G. M., & Gronenborn, A. M. (1992a) *Biochemistry* 31, 3443–3452.  
 Forman-Kay, J. D., Clore, G. M., Stahl, S. J., & Gronenborn, A. M. (1992b) *J. Biomol. NMR* 2, 431–445.  
 Garrett, D. S., Powers, R., Gronenborn, A. M., & Clore, G. M. (1991) *J. Magn. Reson.* 95, 214–220.  
 Hayashi, T., Ueno, Y., & Okamoto, T. (1993) *J. Biol. Chem.* 268, 11380–11388.  
 Holmgren, A. (1985) *Annu. Rev. Biochem.* 54, 237–271.  
 Holmgren, A. (1989) *J. Biol. Chem.* 264, 13963–13966.  
 Jeng, M.-F., Holmgren, A., & Dyson, H. J. (1995) *Biochemistry* 34, 10101–10105.  
 Katti, S., LeMaster, D., & Eklund, A. (1990) *J. Mol. Biol.* 212, 10261–10265.  
 Khoda, D., Sawada, T., & Inagaki, F. (1991) *Biochemistry* 30, 4896–4900.  
 Langsetmo, K., Fuchs, J. A., & Woodward, C. (1991a) *Biochemistry* 30, 7603–7609.  
 Langsetmo, K., Fuchs, J. A., Woodward, C., & Sharp, K. A. (1991b) *Biochemistry* 30, 7609–7614.  
 Matthew, J. B., Gurd, F. R. N., Gracia-Moreno, B., Flannegan, M. A., March, K. L., & Shire, S. J. (1985) *Crit. Rev. Biochem.* 18, 91–197.  
 Matthews, J. R., Wakasugi, N., Virelizier, J. L., Yodoi, J., & Hay, R. T. (1992) *Nucleic Acids Res.* 20, 3821–3830.  
 Mitomo, K., Nakayama, K., Fujimoto, K., Sun, X., Seki, S., & Yamamoto, K. (1994) *Gene* 145, 197–203.  
 Nicholls, A. J., Sharp, K., & Honig, B. (1991) *Proteins* 11, 281–296.  
 Oda, Y., Yamazaki, T., Nagayama, K., Kanaya, S., Kuroda, Y., & Nakamura, H. (1994) *Biochemistry* 33, 5275–5284.  
 Oliveberg, M., Arcus, V. L., & Fersht, A. R. (1995) *Biochemistry* 34, 9424–9433.  
 Powers, R., Gronenborn, A. M., Clore, G. M., & Bax, A. (1991) *J. Magn. Reson.* 94, 209–213.  
 Qin, J., Clore, G. M., & Gronenborn, A. M. (1994) *Structure* 2, 503–521.  
 Qin, J., Clore, G. M., Kennedy, W. M. P., Huth, J. R., & Gronenborn, A. M. (1994) *Structure* 3, 289–297.  
 Saarinen, M., Gleason, F. K., & Eklund, H. (1995) *Structure* 3, 1097–1108.  
 Schaller, W., & Robertson, A. D. (1995) *Biochemistry* 34, 4714–4723.  
 Sharp, K. A., & Honig, B. (1990) *Annu. Rev. Biophys. Biophys. Chem.* 19, 301–332.  
 Szyperski, T., Antuch, W., Schick, M., Betz, A., Stone, S. R., & Wüthrich, K. (1994) *Biochemistry* 33, 9303–9310.  
 Tanford, C. (1962) *Adv. Protein Chem.* 17, 69–165.  
 Toledano, M. B., & Leonard, W. J. (1991) *Proc. Natl. Acad. Sci. U.S.A.* 88, 4328–4332.  
 Warshel, A., & Åquist, J. (1991) *Annu. Rev. Biophys. Biophys. Chem.* 20, 267–298.  
 Wilson, N. A., Barbar, E., Fuchs, J. A., & Woodward, C. (1995) *Biochemistry* 34, 8931–8939.  
 Yamazaki, T., Nicholson, L. K., Wingfield, P. T., Stahl, S. J., Kaufman, J. D., Eyermann, C. J., Hodge, C. N., Lam, P. Y. S., Ru, Y., Jadhav, P. K., Chang, C.-H., Weber, P. C., & Torchia, D. A. (1994) *J. Am. Chem. Soc.* 116, 10791–10792.  
 Yang, A. S., & Honig, B. (1992) *Curr. Opin. Struct. Biol.* 2, 40–45.

BI952299H